

# 000 001 002 003 004 005 006 007 008 009 010 FTP: EFFICIENT PREFILLING FOR LONG-CONTEXT 002 LLM INFERENCE VIA FFN TOKEN PRUNING 003 004 005 006 007 008 009 010

**Anonymous authors**

Paper under double-blind review

## ABSTRACT

Large Language Models (LLMs) have demonstrated remarkable performance across various NLP tasks, and have extended their capability to long-context scenarios. However, the increasing context length leads to longer inference time in both the prefilling and decoding stages. Existing token pruning methods primarily evict tokens to compress the KV cache, and only accelerate the decoding stage. Recent studies have extended token pruning to both stages, but they either yield subtle speedup during the prefilling stage or defer a portion of computations to the decoding phase. Critically, these approaches prioritize the attention module, overlooking the significant computations in the Feed-Forward Network (FFN) module. In this work, we focus on the prefilling stage and propose a novel token pruning method named FTP for long-context LLM inference. Our approach is based on the observation that the FFN module accounts for over 60% of the inference time. FTP reduces this by pruning non-critical tokens before the inference of FFN. The importance of each token, along with the quantity to be pruned, are dynamically determined by the attention scores in each layer. Unlike previous token pruning methods, FTP preserves a substantial amount of information of the pruned tokens through the residual connection, thereby achieving a notable speedup with only a negligible decrease in performance. Specifically, the Qwen2-7B-Instruct model with FTP achieves a speedup of  $1.24\times$  in the prefilling stage with only a 1.30% performance drop compared to the baseline model. The speedup is further boosted to  $1.39\times$  on a Qwen1.5-32B-Chat model. Extensive experiments on long-context datasets across various tasks demonstrate the potential and effectiveness of FTP.

## 033 1 INTRODUCTION 034

035 Large language models (LLMs) have shown remarkable performance in a wide range of natural  
036 language processing applications, including summarization, question-and-answer, dialogue systems,  
037 and contextual learning (Thoppilan et al., 2022; Yuan et al., 2022; Wei et al., 2022; Zhang et al.,  
038 2023a). Recently, long-context models have emerged as an important trend in the development of  
039 LLMs, and several of them have already been launched to process complex and long prompts. For  
040 example, GPT4 (Achiam et al., 2023) and Qwen2 (Yang et al., 2024a) are both capable of 128k  
041 context length, and Claude-3 (Anthropic, 2024) can even process up to 200k tokens.

042 Given the advantages of long-context models, they nevertheless pose enormous challenges at in-  
043 ference time. As depicted in Figure 1, the inference of transformer-based LLMs with a KV cache  
044 typically consists of two stages: 1) the prefilling stage, which applies the self-attention, normaliza-  
045 tion, and the Feed-Forward Network (FFN) modules to all input token parallelly, records the key and  
046 value in the KV cache, and finally produces the first generated token. 2) the decoding stage, which  
047 takes the last generated token as input and iteratively predicts the next token with the input and the  
048 KV cache. We refer to the time spent in the prefilling stage as *time to first token (TTFT)*.

049 While there have been various methods trying to reduce the inference time of long-context LLMs  
050 by pruning the input prompt (Jiang et al., 2023b;a; Pan et al., 2024), compressing the KV cache (Li  
051 et al., 2024; Zandieh et al., 2024), improving the efficiency of decoding (Leviathan et al., 2022; Sun  
052 et al., 2023; Chen et al., 2023), and optimizing the attention kernel with sparse computation (Jiang  
053 et al., 2024), few works (Yang et al., 2024b; Fu et al., 2024) place attention to the reduction of TTFT.  
However, the computationally intensive nature of the prefilling stage implies that the TTFT for long-

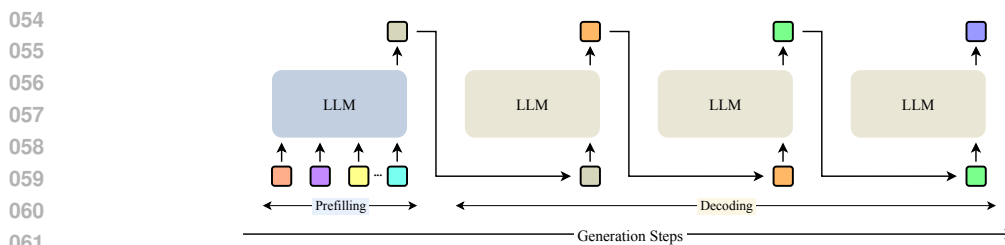


Figure 1: An illustration of the typical inference process of a transformer-based LLM with a KV cache. The first stage is called *prefilling*, which processes all input tokens in parallel and yields the first output token. The second stage is called *decoding*, which iteratively takes the latest generated token as input and generates the subsequent token until the termination condition is satisfied.

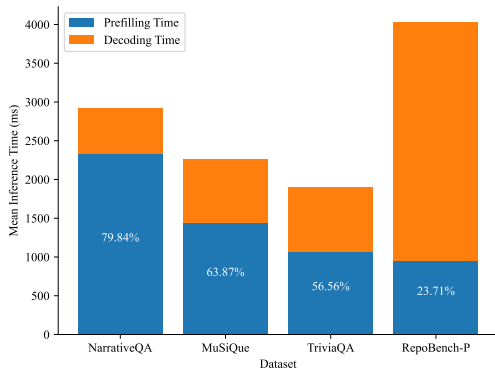


Figure 2: Prefilling proportion during inference. The average prompt lengths are 18409, 11214, 8209, and 4206 respectively. The average generating lengths are 12.08, 16.91, 17.10, and 61.10 respectively.

context inputs is nontrivial. We profile the prefilling and decoding time with the Qwen2-7B-Instruct model on the NarrativeQA (Kočiský et al., 2018), MuSiQue (Trivedi et al., 2022), TriviaQA (Joshi et al., 2017), and the RepoBench-P (Liu et al., 2023) datasets in LongBench (Bai et al., 2023b). For example, in Figure 2, the TTFT accounts for up to 80% of inference time on the NarrativeQA dataset, representing an obstacle to the application of LLMs in long-context scenarios.

To tackle this problem, we focus on the TTFT optimization of long-context LLM inference and propose a novel token pruning method named FFN Token Pruning (FTP) to alleviate computational demands in the prefilling stage. We first investigate the time proportion of the main modules (*i.e.*, the self-attention, normalization, and FFN module) in each layer by conducting experiments on the TriviaQA (Joshi et al., 2017) dataset and profiling the walltime spent on each module. As shown in Figure 3, the FFN module consistently takes a large proportion of inference time on both the Llama3 (AI@Meta, 2024) model and the Qwen2 (Yang et al., 2024a) model, suggesting a large potential for TTFT acceleration by reducing the tokens involving the FFN computation.

Unlike previous token pruning methods (Xiao et al., 2024; Li et al., 2024; Zhang et al., 2023b; Yang et al., 2024b) where tokens are directly pruned from the whole layer, FTP dynamically selects a certain proportion of tokens with an attention-based strategy and prunes them before the inference of FFN. For the pruned tokens, their FFN outputs are logically set to zeros vectors and they remain identical before and after the FFN due to the residual connection. Since the attention scores typically concentrate on a small proportion of tokens, a substantial amount of the FFN calculation can be circumvented, thereby reducing the TTFT. Furthermore, since the attention mechanism of each layer is fully preserved, the underlying context information associated with the tokens is substantially retained, leading to negligible accuracy loss. Extensive experiments on LongBench (Bai et al., 2023b) have demonstrated that our method has a balanced performance both in speedup and accuracy.

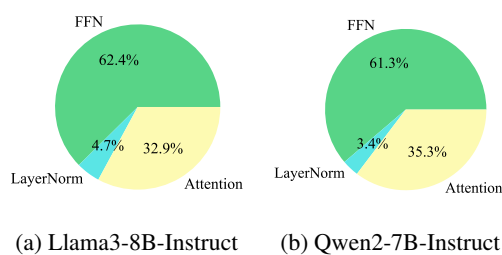


Figure 3: Walltime proportion of the main modules in each decoder layer during prefilling. The time proportion is averaged across all test samples in the TriviaQA dataset.

---

108    

## 2 RELATED WORK

109

110    LLM inference optimization for long-context inputs has emerged as a significant area of NLP re-
111    search. Several prior works (Dao et al., 2022; Kwon et al., 2023; Jiang et al., 2024) directly optimize
112    the computing and memory footprint underlying the common operations in LLMs. In addition to
113    these approaches, a substantial body of work concentrate on the logical inference of the model and
114    optimize the inference process through two kinds of strategies: token pruning and layer skipping.
115

116    

### 2.1 TOKEN PRUNING

117

118    Token pruning for sequence models has become a popular resesearch field before the era of LLM.
119    Ren et al. (2023) proposes a model architecture named SeqBoat to skip non-activated sub-modules.
120    Kim et al. (2022) and Guan et al. (2022) learn certain thresholds or parameterized modules to facil-
121    itate token pruning. For LLMs, many existing works (Liu et al., 2024; Adnan et al., 2024; Nawrot
122    et al., 2024; Feng et al., 2024; Dong et al., 2024) accerlate inference by dropping irrelevant tokens,
123    based on the observation that the attention scores are sparse in most layers. StreamingLLM (Xiao
124    et al., 2024) only preserves the attention sink (*i.e.*, initial tokens) as well as the recent tokens to en-
125    able efficient infinite prompt requests. H2O (Zhang et al., 2023b) introduces the concept of “heavy
126    hitter” and evicts tokens according to the cumulative attention score. SnapKV (Li et al., 2024) votes
127    important previous tokens with the attention scores obtained by the “observation window”, and
128    prunes the unimportant ones to reduce the KV cache used in decoding. While these studies effec-
129    tively compress the computation and memory footprint, they mainly accelerate the decoding phase
130    without reducing the TTFT. On the other hand, PyramidInfer (Yang et al., 2024b) prunes tokens in
131    both the prefilling and decoding phase, only reserving the “pivotal context” tokens in the KV cache.
132    LazyLLM (Fu et al., 2024) also drops tokens from the prefilling stage and proposes an aux cache to
133    avoid redundant computing, enabling the model to pick any subset of the input tokens at each layer,
134    even if some tokens are already pruned. However, these methods either yield subtle speedup during
135    prefilling or defer some computation to the decoding stage. More importantly, they prioritize the
136    attention module and overlook the significant computation demands in the FFN module in practice,
137    where flash attention (Dao et al., 2022) is a prevalent choice for efficient attention computation. Our
138    work accelerates prefilling by pruning non-critical tokens prior to the FFN inference.
139

140    

### 2.2 LAYER SKIPPING

141

142    Layer skipping accelerates the LLM inference by skipping the computation of some decoder layers.
143    LayerSkip (Elhoushi et al., 2024) proposes a layer dropout strategy and an early exit loss during
144    training, enabling layer skipping during inference, without a significant accuracy drop. MoD (Ra-
145    poso et al., 2024) learns a router to determine for a token whether to skip both the self-attention and
146    MLP blocks in a layer. Tyukin et al. (2024) investigates three types of layer skipping: 1) skipping
147    MLP layers, 2) skipping attention layers, and 3) skipping transformer blocks on the 7B and 13B
148    Llama2 Touvron et al. (2023) models, and observes that dropping the attention modules leads to
149    much lower decrease in performance than dropping the FFN modules. Although our work focuses
150    on reducing the computation in the FFN modules, the modules are not entirely bypassed, which
151    results in slight degradation in performance.
152

153    

## 3 FTP

154

155    

### 3.1 LLM INFERENCE PERFORMANCE ANALYSIS

156

157    The inference of common LLMs comprises two phases: *prefilling* and *decoding*. The prefilling
158    phase processes all prompt tokens in parallel, involving numerous GEMM operations, while the
159    decoding phase iteratively takes the last generated token as input and predicts the next token until
160    the stop condition is met.
161

162    As most existing LLMs utilize the transformer architecture, their inference process usually involves
163    the forward of the stack of decoder layers, each of which mainly consists of three modules: nor-
164    malization, self-attention and feed-forward network (FFN). As shown in Figure 3, the FFN module
165    takes up over 60% of walltime of each decoder layer, highlighting a clear opportunity for accel-
166

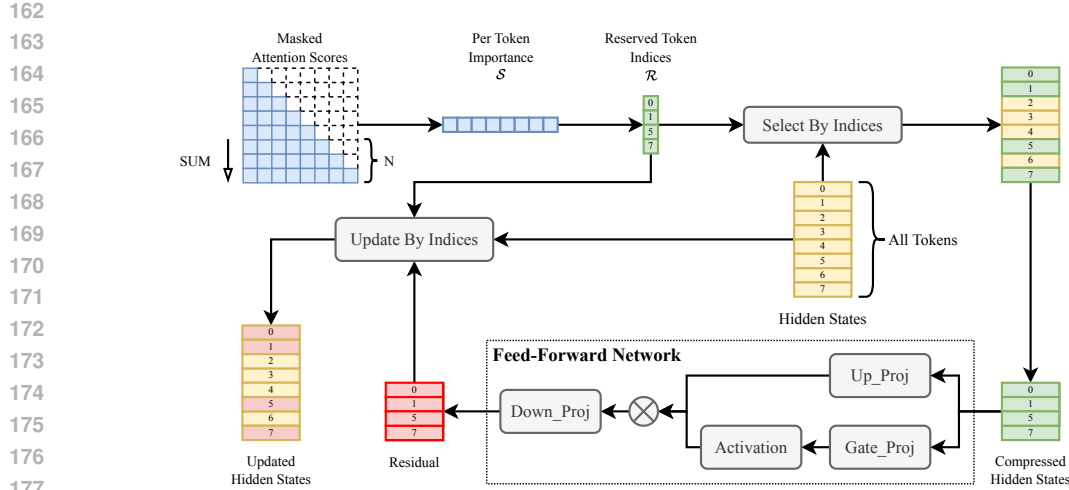


Figure 4: Overview of FTP in a layer. FTP starts from the end of the self-attention module. First, FTP obtains the attention scores from the last  $N$  queries to all keys, and sums them in the *head* and *query* dimension (note that the *head* dimension is omitted in the figure) to derive the importance score  $S$  for each token. Next, the indices  $\mathcal{R}$  of the tokens to prune are determined via Equation 2. Then token selection is performed based on  $\mathcal{R}$ , and only the chosen tokens are processed through the FFN. Finally, the FFN results (*i.e.*, residual) are utilized to update the corresponding token as specified by  $\mathcal{R}$ , while the unimportant tokens are not updated during the FFN inference in this layer.

eration. Taking two commonly encountered models, Llama3 (AI@Meta, 2024) and Qwen2 (Yang et al., 2024a), as examples, the FFN module takes the features of a sequence of  $L$  tokens  $\mathcal{T} \in \mathbb{R}^{L \times C}$  as input, and processes them token-wisely according to the function below:

$$FFN(\mathcal{T}) = (\mathcal{T}'W_U \odot A(\mathcal{T}'W_G))W_D, \quad (1)$$

where  $\mathcal{T}' = Norm(\mathcal{T})$  are the normalized features,  $A(\cdot)$  refers to the activation function (*e.g.*, SiLU (Elfwing et al., 2018) in Llama3), and  $W_D \in \mathbb{R}^{I \times C}$ ,  $W_U \in \mathbb{R}^{C \times I}$ ,  $W_G \in \mathbb{R}^{C \times I}$  refers to the *Down Projection*, *Up Projection* and *Gate Projection* matrices respectively. The formula indicates that most operations of FFN take place in the large and dense matrix multiplication with the three weight matrices, and the total FLOPs of these three matrix multiplication sum up to  $6LCI$  (*i.e.*,  $2LCI$  for one matrix multiplication). Note that other LLMs probably have slightly different FFN architectures, but the most computationally expensive part of theirs are still the matrix multiplication, which matches our analysis. Since both the hidden size of tokens (*i.e.*,  $C$ ) and the size of weight matrices (*i.e.*,  $C$  and  $I$ ) are fixed in an off-the-shelf model, reducing the sequence length  $L$  emerges as a viable strategy for FFN acceleration.

### 3.2 TOKEN PRUNING FOR FFN

Based on the analysis above, in this work, we propose to reduce the number of tokens before feeding them into FFN to accelerate the prefilling stage. Let us denote the “important” and “unimportant” sets of tokens as  $\mathcal{T}_I \in \mathbb{R}^{L_I \times C}$  and  $\mathcal{T}_U \in \mathbb{R}^{L_U \times C}$ , where  $L_I$  and  $L_U$  are the number of “important” and “unimportant” tokens. As shown in Figure 4, only the “important” tokens are involved in the FFN calculation as formulated in Equation 1, and the FFN results for the “unimportant” tokens are logically set to zero vectors (*i.e.*,  $FFN(\mathcal{T}_U) = 0$ ). Thanks to the residual connection surrounding the FFN module, setting the FFN results to be zeros vectors is equivalent to bypassing the updates in the FFN. Consequently, the FLOPs required for the FFN are reduced to  $6L_I CI$  from  $6LCI$ .

To this end, two critical questions arise: 1) how to divide the input tokens into “important” and “unimportant” ones, and 2) how many tokens could be pruned, without causing obvious harm to the model performance? We analyse and discuss them in the following Section 3.2.1 and Section 3.2.2.

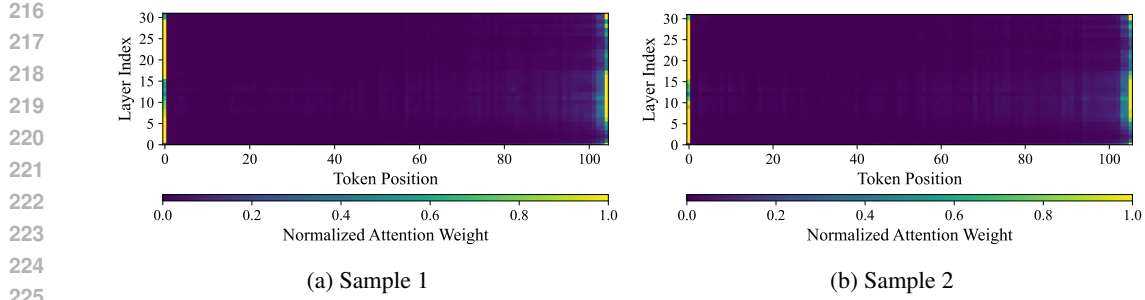


Figure 5: Visualization of the normalized attention weight for each layer. The experiment is conducted on a Llama3-8B-Instruct model on the Qasper dataset. Since the input length is too long to visualize, we divide the tokens into several groups with a group size of 32. Each column in the graph represents the average attention weight of a group of tokens across all layers. More visualization of the samples is in Appendix 6.2.

### 3.2.1 TOKEN PRUNING WITH ATTENTION SCORE

Token pruning is a common method to compress the input to LLM modules. Many existing works (Li et al., 2024; Fu et al., 2024; Yang et al., 2024b) propose to evaluate the importance of tokens with either the exact attention score matrix (*i.e.*,  $\text{softmax}(\frac{QK^T}{\sqrt{d_k}})$ ) or an estimated one. Inspired by these studies and the computational order of self-attention and the FFN module, we propose to evaluate the importance of the tokens with the attention score from the current layer.

To investigate whether the attention score is suitable for token pruning for FFN, we visualize the attention score of layers from different depths in the Llama3-8B-Instruct (AI@Meta, 2024) model. As shown in Figure 5, we discover that 1) the attention scores in each layer are typically concentrated on a small number of tokens; 2) tokens with high attention scores in one layer may not necessarily be prioritized in the same manner across other layers; 3) the number of tokens with high attention scores varies among different layers.

Based on these observations, we propose an attention-based approach to evaluate the importance of the tokens in each layer. Let us denote the attention score matrices for all attention heads as  $\mathcal{M} = \{M_h \in \mathbb{R}^{L \times L}\}_{h=1}^H = \{\text{softmax}(\frac{Q_h K_h^T}{\sqrt{d_k}})\}_{h=1}^H$ , where  $H$  is the number of attention heads. Since prior work (Li et al., 2024) has empirically revealed that the attention pattern obtained by the queries at the end of the prompts is nearly consistent with that obtained by all queries, we only retain the attention scores  $\mathcal{M}'$  from the last  $N$  queries to reduce overhead (*i.e.*,  $\mathcal{M}' = \{M'_h \in \mathbb{R}^{N \times L}\}_{h=1}^H$ ). The attention scores  $\mathcal{M}'$  are summed over all heads and queries to form the importance score  $\mathcal{S}$  for each token. Inspired by Xiao et al. (2024), we statically reserve the initial  $P$  and the last  $N$  tokens in the prompts to maintain accuracy. These tokens are excluded from  $\mathcal{S}$ , resulting in the length of  $\mathcal{S}$  being  $L - P - N$ . After that, the reserved token indices  $\mathcal{R}$  can be calculated as

$$\begin{aligned} \mathcal{R} = & \{i | i \in \mathbb{Z} \wedge 1 \leq i \leq P\} \\ & \cup \{i + P | i \in \Gamma(\mathcal{S}, k)\} \\ & \cup \{i | i \in \mathbb{Z} \wedge L - N < i \leq L\}, \end{aligned} \quad (2)$$

$$k = \min_{\sum_{i \in \Gamma(S, n)} S_i >= \eta \sum_i S_i} n, \quad (3)$$

where  $\Gamma(A, a)$  returns the set of indices corresponding to the top  $a$  elements in vector  $A$ . In this way, we reserve the top  $k$  tokens such that their proportions of importance scores sums up to the reserve ratio  $\eta$ , as well as the initial  $P$  and last  $N$  tokens. The pseudo-code for FTP is in Algorithm 1.

Given that the attention scores tend to concentrate on a small number of tokens, a substantial number of tokens can be pruned in each layer even when  $\eta$  approaches to 1.0. More importantly, the importance score  $S$  is computed with little overhead at each layer, which alleviates the problem reflected by the second observation. Since we use a reserved ratio  $\eta$  rather than a static number to determine the number of tokens to retain, our approach is capable of handling various distributions of attention scores in different layers, as revealed in the third observation.

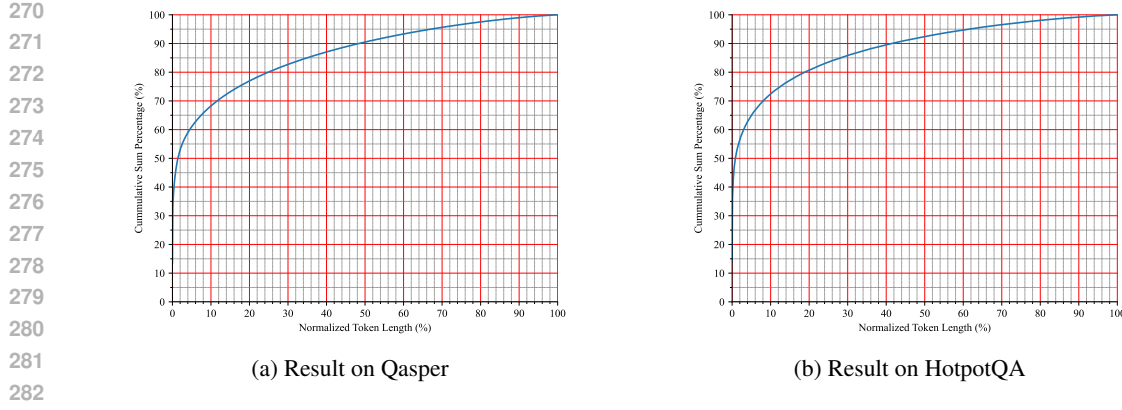


Figure 6: The cumulative percentage of attention scores w.r.t. the normalized token length. The experiments are conducted on the Qasper (Dasigi et al., 2021) and HotpotQA (Yang et al., 2018) dataset with a Llama3-8B model. The results are averaged among all decoder layers and all samples.

### 3.2.2 TOKEN PRUNING PROPORTION

Since the number of pruned tokens is determined by the reserved ratio  $\eta$  in each layer, we quantitatively investigate the relationship between  $\eta$  and the number of reserved tokens by conducting an experiment on the Qasper (Dasigi et al., 2021) and HotpotQA (Yang et al., 2018) dataset with a Llama3-8B (AI@Meta, 2024) model. Concretely, we first derive the attention score matrices at each layer, average the scores along the *head* and *query* dimension, and obtain the averaged attention score for each token at each layer. Next, for each layer, we sort the tokens descendingly by their averaged attention score. Then we uniformly divide the input length into 100 steps, and record the cumulative percentage of attention score at each step. Finally, we average the cumulative percentage over all layers and all samples in the dataset, and the result is depicted in Figure 6. As shown in the result, a large proportion of attention score (*i.e.*, 95%) is occupied by only 60% of tokens, which is consistent with the first observation in Section 3.2.1, and suggests an opportunity for token pruning.

On the other hand, we empirically discover that shallow layers are more sensitive to our FTP (see Section 4.6), which is consistent with the conclusions of previous works (Fu et al., 2024; Yang et al., 2024b). However, we propose to preserve the whole layer (*i.e.*,  $\eta = 1.0$ ) for the first  $\mathcal{F}$  layers, and apply token pruning to the following layers. Thanks to the high pruning efficiency of FTP, the model maintains a considerable overall pruning rate.

---

#### Algorithm 1 PyTorch Pseudo Code for FTP

---

**Input:** current layer index  $c$ , hidden state  $X$ , number of attention heads  $H$ ,  $\eta$ ,  $\mathcal{F}$ ,  $L$ ,  $P$  and  $N$   
 1:  $\mathcal{O}, \mathcal{M} = \text{self-attention}(X)$   
 2: **if**  $c > \mathcal{F}$  **then**  
 3:      $\mathcal{S} = \mathcal{M}.\text{sum}(0).\text{sum}(0)[P:-N]$  # Assume  $\mathcal{M}$  has a size of  $(H, L, L)$   
 4:     score, idx =  $\text{sort}(\mathcal{S}, \text{descending=True})$   
 5:     cumSum =  $\text{cumsum}(\text{score})$   
 6:     threshold =  $\text{cumSum}[-1] * \eta$   
 7:     n =  $\text{where}(\text{cumSum} > \text{threshold})[0] + 1$  # The first index that meets the condition  
 8:     idx =  $\text{idx}[:n] + P$  # Select the top  $n$  indices and shift them by  $P$   
 9:      $\mathcal{R} = \text{cat}(\text{arange}(P), \text{idx}, \text{arange}(L - N, L))$   
 10:    residual =  $\text{FFN}(\mathcal{O}[\mathcal{R}, :])$   
 11:     $\mathcal{O}[\mathcal{R}, :] += \text{residual}$   
 12: **else**  
 13:    residual =  $\text{FFN}(\mathcal{O})$   
 14:     $\mathcal{O} += \text{residual}$   
 15: **end if**  
**Output:** Output hidden state  $\mathcal{O}$

---

Tasks	Method	Llama3-8B-Instruct		Qwen2-7B-Instruct	
		Score	TTFT Speedup ( $\times$ )	Score	TTFT Speedup ( $\times$ )
Single-Document QA	Baseline	<b>37.20</b>	1.00	<b>39.00</b>	1.00
	LLMLingua2	29.29	0.71	30.24	0.98
	PyramidInfer*	31.33	0.56	/	/
	PyramidInfer	32.05	1.02	29.19	1.21
	Ours	36.06	<b>1.20</b>	38.75	<b>1.22</b>
Multi-Document QA	Baseline	<b>36.85</b>	1.00	<b>37.48</b>	1.00
	LLMLingua2	30.43	0.72	31.38	1.10
	PyramidInfer*	33.92	0.53	/	/
	PyramidInfer	33.43	0.97	32.86	1.19
	Ours	34.85	<b>1.21</b>	35.21	<b>1.26</b>
Summarization	Baseline	<b>26.80</b>	1.00	<b>26.70</b>	1.00
	LLMLingua2	23.83	0.73	23.54	1.01
	PyramidInfer*	24.20	0.62	/	/
	PyramidInfer	24.21	1.06	22.65	1.20
	Ours	24.41	<b>1.19</b>	25.01	<b>1.23</b>
Few-shot Learning	Baseline	<b>69.33</b>	1.00	<b>70.17</b>	1.00
	LLMLingua2	38.73	0.82	42.88	1.08
	PyramidInfer*	66.69	0.53	/	/
	PyramidInfer	66.37	0.97	66.10	1.24
	Ours	67.55	<b>1.21</b>	69.11	<b>1.25</b>
Synthetic	Baseline	<b>37.00</b>	1.00	<b>37.50</b>	1.00
	LLMLingua2	12.75	0.66	7.75	1.10
	PyramidInfer*	36.00	0.50	/	/
	PyramidInfer	35.50	0.94	35.50	1.16
	Ours	36.00	<b>1.25</b>	36.75	<b>1.30</b>
Code Completion	Baseline	55.17	1.00	<b>58.43</b>	1.00
	LLMLingua2	31.47	0.69	37.69	0.88
	PyramidInfer*	<b>55.29</b>	0.66	/	/
	PyramidInfer	55.24	1.10	56.52	<b>1.24</b>
	Ours	35.91	<b>1.19</b>	56.74	1.22

Table 1: TTFT speedup and accuracy score across various long-context tasks on LongBench. The result for each task is computed by averaging the results of datasets belonging to the task. Note that the attention modules of all methods except for PyramidInfer\* are implemented with flash attention, which is lossless in accuracy and efficient in time and memory, while PyramidInfer\* is the official implementation with PyTorch-implemented attention. Additionally, PyramidInfer\* encounters out-of-memory issues when applied to the Qwen2 model, which has a max context length of 32k.

## 4 EXPERIMENTS

**Datasets.** We conduct experiments on the LongBench (Bai et al., 2023b) benchmark, containing 16 long-context datasets for 6 types of tasks (*i.e.*, single-document QA, multi-document QA, summarization, few-shot learning, synthetic tasks, and code completion), which provides a comprehensive assessment on the long-context understanding capability of LLMs. The average context length across the datasets ranges from 5,000 to 15,000, with the number of test samples in each dataset typically being 200, except for the datasets of code completion, which contain 500 samples. We follow the official pipeline of LongBench to pre-process the data and evaluate the models.

**Metrics.** We utilize two kinds of metrics to assess the quality and efficiency of the generating process of the LLMs with our proposed FTP. The quality metric is the accuracy score from LongBench. Since the datasets in LongBench adopt various metrics for the accuracy evaluation, the accuracy score for each dataset is one of the following metrics: 1) F1 Score, 2) Rouge-L, 3) Accuracy, and 4) Edit Similarity. All of these metrics have a range from 0.0 to 1.0, hence we average them to represent the accuracy score of a task. The efficiency metric is the TTFT speedup (*i.e.*  $\frac{TTFT_{baseline}}{TTFT_{FTP}}$ ) w.r.t. the baseline model (*i.e.*, inferencing the pre-trained model with the standard process).

378  
379

## 4.1 IMPLEMENTATION DETAILS

380  
381  
382  
383  
384  
385  
386  
387  
388

**Basic Configuration.** We implement FTP on the Llama3-8B-Instruct (AI@Meta, 2024), Qwen2-7B-Instruct (Yang et al., 2024a) and two larger models (see Section 4.5). The max context length for Qwen2 and Llama3 are 32k and 8k respectively, and the data samples that exceed the max context length of the models are truncated during the data pre-processing pipeline of LongBench. We set  $P = 100$  and  $N = 50$  for both models. For the Llama3-8B model, we set  $\mathcal{F} = 10$  to preserve the first 10 layers and  $\eta = 0.90$  for the following layers. When it comes to the Qwen2-7B model,  $\mathcal{F}$  and  $\eta$  are set as 10 and 0.95 respectively. Note that FTP is free of further training and shares the same weights with the original model. All experiments are conducted on NVIDIA A100 GPUs without model quantization.

389  
390  
391  
392

**Attention Implementation.** Our method is implemented with the transformers library (Wolf et al., 2020) and flash attention, which is a prevalent choice in practical inference of LLMs. Given that flash attention inherently does not return attention weights, we recalculate the necessary attention weights to assess token importance, introducing only a negligible cost (refer to Section 4.6.1).

393  
394

## 4.2 RESULTS ON LONGBENCH

395  
396  
397  
398  
399  
400

We conduct experiments on LongBench (Bai et al., 2023b), including six long-context tasks, to evaluate the accuracy score and TTFT speedup of our method. In addition to the baseline model, we incorporate a state-of-the-art prompt compression method (Pan et al., 2024) for comparison, which formulates prompt compression as a token classification problem and utilizes a transformer encoder with a linear classification head to prune the prompt before feeding them into the LLM.

401  
402  
403  
404  
405  
406  
407

The performance for each task is calculated by averaging the results of datasets associated with that specific task. As shown in Table 1, FTP generally presents considerable speedup across all six long-context tasks with a negligible drop in accuracy score. Thanks to the longer context support (*i.e.*, 32k) of Qwen2-7B-Instruct, FTP achieves even greater speed improvements, despite applying a higher reserved ratio  $\eta$ . Furthermore, LLMLingua2 (Pan et al., 2024) on both models can hardly accelerate the pre-filling stage even with a compression ratio of 0.2.

408

## 4.3 COMPARISON WITH STATE-OF-THE-ART METHOD

409  
410  
411  
412

We conduct a comparative analysis between FTP and PyramidInfer (Yang et al., 2024b), a state-of-the-art method of prefilling acceleration. PyramidInfer accelerates both the prefilling and decoding stages by compressing the KV cache with different compression rates for each layer.

413  
414  
415  
416  
417  
418  
419  
420  
421

We conduct experiments on the Llama3-8B-Instruct and Qwen2-7B-Instruct models, and the results are in Table 1. We present two versions of PyramidInfer for comparison. The official implementation of PyramidInfer (denoted as PyramidInfer\* in Table 1) utilizes PyTorch-implemented attention module and fails to accelerate the prefilling stage. Furthermore, it encounters out-of-memory issues when applied to the Qwen2 model, which has a max context length of 32k. On the other hand, we re-implement PyramidInfer (denoted as PyramidInfer in Table 1) with flash attention and re-calculate the necessary attention weights (*i.e.*, 20% attention weights following the official setting) for it. At this time, PyramidInfer gets rid of out-of-memory issues on Qwen2 model but is still slower with more accuracy degradation than FTP in most tasks.

422  
423

## 4.4 ACCURACY VS. TTFT SPEEDUP

424  
425  
426  
427  
428  
429  
430  
431

The TTFT speedup of FTP can be modulated from two aspects: 1) the number of layers to which FTP is applied, and 2) the reserved ratio  $\eta$  at each decoder layer. We further examine the variation of accuracy score *w.r.t.* TTFT speedup by evaluating the accuracy score at various levels of inference efficiency. We incorporate LLMLingua-2 for comparison and adjust the prompt compression rate to achieve different speedups. As shown in Figure 7, FTP achieves notable TTFT speedup with negligible performance drop across various tasks, presenting an effective balance between speedup and accuracy. Moreover, the accuracy score of FTP even surpasses that of the baseline in certain tasks (*e.g.*, Single-Document QA and Synthetic Task). Conversely, LLMLingua2 experiences an evident decline in accuracy to accelerate the prefilling stage.

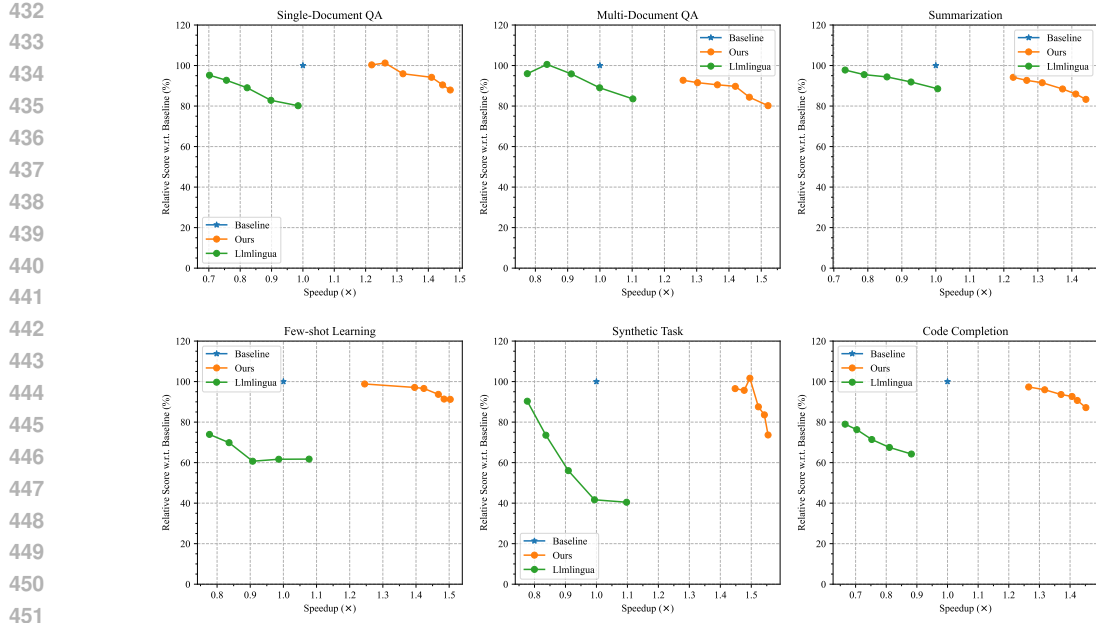


Figure 7: TTFT speedup vs. accuracy comparison for Qwen2-7B-Instruct across different tasks.

#### 455 4.5 FTP ON LARGER MODELS

456  
457 In this section, we further investigate the effectiveness of FTP on larger LLMs and evaluate our  
458 model on Qwen1.5-32B-Chat (Bai et al., 2023a) and Qwen2-72B-Instruct (Yang et al., 2024a),  
459 both of which support a max context length of 32k. For the Qwen1.5-32B-Chat model, we preserve  
460 the first  $\mathcal{F} = 10$  layers and set  $\eta = 0.90$  for the subsequent 54 layers. For the Qwen2-72B-Instruct  
461 model, we preserve the first  $\mathcal{F} = 10$  and set  $\eta = 0.93$  for the following 70 layers. As shown in  
462 Table 2, FTP facilitates a significant speedup across all tasks with a subtle impact on the accuracy  
463 score, which indicates the potential of practical application of FTP.

464 We attribute this enhanced acceleration on the larger models to two primary factors. Firstly, larger  
465 models have deeper architectures. Therefore, compared to the smaller models, more tokens can be  
466 pruned even though the first  $\mathcal{F}$  layers are fully preserved. Secondly, these models have up to  $4\times$  and  
467 even  $10\times$  of weights, and they exhibit robustness on accuracy even when a substantial number of  
468 tokens are pruned.

470 Tasks	471 Method	472 Qwen1.5-32B-Chat		473 Qwen2-72B-Instruct	
		474 Score	475 TTFT Speedup (x)	476 Score	477 TTFT Speedup (x)
478 Single-Document QA	Baseline	<b>40.68</b>	1.00	<b>43.78</b>	1.00
	Ours	37.16	<b>1.37</b>	41.36	<b>1.31</b>
480 Multi-Document QA	Baseline	<b>44.98</b>	1.00	<b>62.70</b>	1.00
	Ours	42.06	<b>1.39</b>	60.92	<b>1.33</b>
482 Summarization	Baseline	<b>25.91</b>	1.00	<b>28.32</b>	1.00
	Ours	23.78	<b>1.37</b>	26.80	<b>1.32</b>
484 Few-shot Learning	Baseline	66.99	1.00	<b>69.87</b>	1.00
	Ours	<b>67.74</b>	<b>1.40</b>	67.15	<b>1.33</b>
486 Synthetic	Baseline	<b>52.67</b>	1.00	<b>54.50</b>	1.00
	Ours	46.25	<b>1.45</b>	51.00	<b>1.34</b>
488 Code Completion	Baseline	<b>46.97</b>	1.00	<b>69.05</b>	1.00
	Ours	46.63	<b>1.39</b>	68.35	<b>1.36</b>

Table 2: TTFT speedup and accuracy on various tasks on Qwen1.5-32B and Qwen2-72B models.

486    4.6 ABLATION STUDY  
 487

488    We conduct an ablation study of FTP on the approaches and hyper-parameters we proposed in Sec-  
 489    tion 3.2. The experiment for our token pruning strategy is in Section 4.6.1, and more analysis can  
 490    be found in Appendix 6.1.  
 491

492    4.6.1 TOKEN PRUNING STRATEGY  
 493

494    To evaluate the token pruning strategy proposed in Section 3.2.1, we replace our attention-based  
 495    strategy with a random selecting strategy and evaluate the model performance with Llama3-8B-  
 496    Instruct and Qwen2-7B-Instruct. Concretely, we first record the number of pruned tokens in each  
 497    layer for each sample in our approach, and then randomly prune the same number of tokens in the  
 498    “random” variant. As illustrated in Table 3, our attention-based strategy is crucial in determining  
 499    which tokens to prune. The model accuracy consistently suffers a significant drop across all tasks  
 500    when applied a random pruning strategy. On the other hand, the TTFT of FTP is only marginally  
 501    higher than that of the random variant, indicating that the computational cost introduced by FTP is  
 502    trivial. Specifically, the computational cost introduced by FTP on Llama3 and Qwen2 models are  
 503    7-10ms and 8-15ms respectively, accounting for only 1%-3% and 0.8%-1.9% of the TTFT.  
 504

Tasks	Method	Llama3-8B-Instruct		Qwen2-7B-Instruct	
		Score	TTFT (ms)	Score	TTFT (ms)
Single-Document QA	Baseline	<b>37.20</b>	574.70	<b>39.00</b>	1122.30
	Random	11.14	469.99	20.63	907.75
	Ours	36.06	480.24	38.75	923.18
Multi-Document QA	Baseline	<b>36.85</b>	664.80	<b>37.48</b>	1080.73
	Random	7.56	541.11	9.82	845.63
	Ours	34.85	551.23	35.21	859.11
Summarization	Baseline	<b>26.80</b>	526.11	<b>26.70</b>	797.57
	Random	15.90	428.95	18.67	636.32
	Ours	24.41	438.08	25.01	647.59
Few-shot Learning	Baseline	<b>69.33</b>	594.20	<b>70.17</b>	810.22
	Random	21.58	481.82	33.81	630.81
	Ours	67.55	489.26	69.11	641.58
Synthetic	Baseline	<b>37.00</b>	732.98	<b>37.50</b>	1235.10
	Random	2.72	573.84	1.71	947.67
	Ours	36.00	584.18	36.75	955.94
Code Completion	Baseline	<b>55.17</b>	449.45	<b>58.43</b>	621.11
	Random	16.28	367.09	24.41	489.04
	Ours	35.91	375.22	56.74	498.15

525    Table 3: Accuracy and TTFT comparison for Llama3-8B-Instruct and Qwen2-7B-Instruct employ-  
 526    ing random pruning strategy and our attention-based strategy. The *random* variant prunes the iden-  
 527    tical number of tokens at each layer as ours.  
 528

529    5 CONCLUSION  
 530

532    In this work, we explore a novel approach of prefilling acceleration by pruning tokens for FFN, and  
 533    propose the FFN Token Pruning (FTP) technique for long-context inference of LLMs, without addi-  
 534    tional training or finetuning. We start by analyzing the TTFT proportion in long-context inference of  
 535    LLMs, and profiling the time proportion of the primary components in a typical LLM layer. Observ-  
 536    ing the substantial time allocation to FFN during prefilling, we reduces FFN computation time by  
 537    “pruning” non-critical tokens with an attention-based strategy prior to FFN inference. In a addition,  
 538    FTP preserves a large amount of information of the pruned toknes through the residual connection.  
 539    Experiments on long-context datasets across various tasks indicate that FTP is capable of delivering  
 significant acceleration while maintaining performance.

540 REFERENCES  
541

- 542 Josh Achiam, Steven Adler, Sandhini Agarwal, Lama Ahmad, Ilge Akkaya, Florencia Leoni Ale-  
543 man, Diogo Almeida, Janko Altenschmidt, Sam Altman, Shyamal Anadkat, et al. Gpt-4 technical  
544 report. *arXiv preprint arXiv:2303.08774*, 2023.
- 545 Muhammad Adnan, Akhil Arunkumar, Gaurav Jain, Prashant Nair, Ilya Soloveychik, and Pu-  
546 rushotham Kamath. Keyformer: Kv cache reduction through key tokens selection for efficient  
547 generative inference. *Proceedings of Machine Learning and Systems*, 6:114–127, 2024.
- 548 AI@Meta. Llama 3 model card. 2024. URL [https://github.com/meta-llama/llama3/blob/main/MODEL\\_CARD.md](https://github.com/meta-llama/llama3/blob/main/MODEL_CARD.md).
- 549 Chenxin An, Shansan Gong, Ming Zhong, Mukai Li, Jun Zhang, Lingpeng Kong, and Xipeng Qiu.  
550 L-eval: Instituting standardized evaluation for long context language models, 2023.
- 551 Anthropic. The claude 3 model family: Opus, sonnet, haiku, 2024. URL [https://www-cdn.anthropic.com/de8ba9b01c9ab7cbabf5c33b80b7bbc618857627/Model\\_Card\\_Claude\\_3.pdf](https://www-cdn.anthropic.com/de8ba9b01c9ab7cbabf5c33b80b7bbc618857627/Model_Card_Claude_3.pdf).
- 552 Jinze Bai, Shuai Bai, Yunfei Chu, Zeyu Cui, Kai Dang, Xiaodong Deng, Yang Fan, Wenbin Ge,  
553 Yu Han, Fei Huang, Bin Yuan Hui, Luo Ji, Mei Li, Junyang Lin, Runji Lin, Dayiheng Liu, Gao Liu,  
554 Chengqiang Lu, Keming Lu, Jianxin Ma, Rui Men, Xingzhang Ren, Xuancheng Ren, Chuanqi  
555 Tan, Sinan Tan, Jianhong Tu, Peng Wang, Shijie Wang, Wei Wang, Shengguang Wu, Benfeng  
556 Xu, Jin Xu, An Yang, Hao Yang, Jian Yang, Shusheng Yang, Yang Yao, Bowen Yu, Hongyi  
557 Yuan, Zheng Yuan, Jianwei Zhang, Xingxuan Zhang, Yichang Zhang, Zhenru Zhang, Chang  
558 Zhou, Jingren Zhou, Xiaohuan Zhou, and Tianhang Zhu. Qwen technical report. *arXiv preprint  
559 arXiv:2309.16609*, 2023a.
- 560 Yushi Bai, Xin Lv, Jiajie Zhang, Hongchang Lyu, Jiankai Tang, Zhidian Huang, Zhengxiao Du,  
561 Xiao Liu, Aohan Zeng, Lei Hou, et al. Longbench: A bilingual, multitask benchmark for long  
562 context understanding. *arXiv preprint arXiv:2308.14508*, 2023b.
- 563 Charlie Chen, Sebastian Borgeaud, Geoffrey Irving, Jean-Baptiste Lespiau, L. Sifre, and John M.  
564 Jumper. Accelerating large language model decoding with speculative sampling. *ArXiv*,  
565 abs/2302.01318, 2023. URL <https://api.semanticscholar.org/CorpusID:256503945>.
- 566 Karl Cobbe, Vineet Kosaraju, Mohammad Bavarian, Mark Chen, Heewoo Jun, Lukasz Kaiser,  
567 Matthias Plappert, Jerry Tworek, Jacob Hilton, Reiichiro Nakano, Christopher Hesse, and John  
568 Schulman. Training verifiers to solve math word problems. *arXiv preprint arXiv:2110.14168*,  
569 2021.
- 570 Tri Dao, Daniel Y. Fu, Stefano Ermon, Atri Rudra, and Christopher Ré. FlashAttention: Fast and  
571 memory-efficient exact attention with IO-awareness. In *Advances in Neural Information Processing  
572 Systems (NeurIPS)*, 2022.
- 573 Pradeep Dasigi, Kyle Lo, Iz Beltagy, Arman Cohan, Noah A. Smith, and Matt Gardner. A  
574 dataset of information-seeking questions and answers anchored in research papers. In *Proceed-  
575 ings of the 2021 Conference of the North American Chapter of the Association for Compu-  
576 tational Linguistics: Human Language Technologies*, pp. 4599–4610, Online, June 2021. Asso-  
577 ciation for Computational Linguistics. doi: 10.18653/v1/2021.nacl-main.365. URL <https://aclanthology.org/2021.nacl-main.365>.
- 578 Harry Dong, Xinyu Yang, Zhenyu Zhang, Zhangyang Wang, Yuejie Chi, and Beidi Chen. Get more  
579 with less: Synthesizing recurrence with kv cache compression for efficient llm inference, 2024.
- 580 Stefan Elfwing, Eiji Uchibe, and Kenji Doya. Sigmoid-weighted linear units for neural network  
581 function approximation in reinforcement learning. *Neural networks*, 107:3–11, 2018.
- 582 Mostafa Elhoushi, Akshat Shrivastava, Diana Liskovich, Basil Hosmer, Bram Wasti, Liangzhen Lai,  
583 Anas Mahmoud, Bilge Acun, Saurabh Agarwal, Ahmed Roman, Ahmed A Aly, Beidi Chen, and  
584 Carole-Jean Wu. Layerskip: Enabling early exit inference and self-speculative decoding, 2024.  
585 URL <https://arxiv.org/abs/2404.16710>.

- 594 Yuan Feng, Junlin Lv, Yukun Cao, Xike Xie, and S. Kevin Zhou. Ada-kv: Optimizing kv cache  
 595 eviction by adaptive budget allocation for efficient llm inference, 2024. URL <https://arxiv.org/abs/2407.11550>.
- 596
- 597 Qichen Fu, Minsik Cho, Thomas Merth, Sachin Mehta, Mohammad Rastegari, and Mahyar Najibi.  
 598 Lazyllm: Dynamic token pruning for efficient long context llm inference, 2024. URL <https://arxiv.org/abs/2407.14057>.
- 599
- 600
- 601 Yue Guan, Zhengyi Li, Jingwen Leng, Zhouhan Lin, and Minyi Guo. Transkimmer: Transformer  
 602 learns to layer-wise skim. *arXiv preprint arXiv:2205.07324*, 2022.
- 603
- 604 Huiqiang Jiang, Qianhui Wu, , Xufang Luo, Dongsheng Li, Chin-Yew Lin, Yuqing Yang, and Lili  
 605 Qiu. Longllmlingua: Accelerating and enhancing llms in long context scenarios via prompt com-  
 606 pression. *ArXiv preprint*, abs/2310.06839, 2023a. URL <https://arxiv.org/abs/2310.06839>.
- 607
- 608
- 609 Huiqiang Jiang, Qianhui Wu, Chin-Yew Lin, Yuqing Yang, and Lili Qiu. LLMLingua: Compressing  
 610 prompts for accelerated inference of large language models. In *Proceedings of the 2023 Confer-  
 611 ence on Empirical Methods in Natural Language Processing*, pp. 13358–13376. Association for  
 612 Computational Linguistics, December 2023b. doi: 10.18653/v1/2023.emnlp-main.825. URL  
 613 <https://aclanthology.org/2023.emnlp-main.825>.
- 614
- 615 Huiqiang Jiang, Yucheng Li, Chengruidong Zhang, Qianhui Wu, Xufang Luo, Surin Ahn, Zhen-  
 616 hua Han, Amir H Abdi, Dongsheng Li, Chin-Yew Lin, Yuqing Yang, and Lili Qiu. Minference  
 617 1.0: Accelerating pre-filling for long-context llms via dynamic sparse attention. *arXiv preprint  
 618 arXiv:2407.02490*, 2024.
- 619
- 620 Mandar Joshi, Eunsol Choi, Daniel Weld, and Luke Zettlemoyer. TriviaQA: A large scale distantly  
 621 supervised challenge dataset for reading comprehension. In Regina Barzilay and Min-Yen Kan  
 622 (eds.), *Proceedings of the 55th Annual Meeting of the Association for Computational Linguistics  
 623 (Volume 1: Long Papers)*, pp. 1601–1611, Vancouver, Canada, July 2017. Association for Com-  
 624 putational Linguistics. doi: 10.18653/v1/P17-1147. URL <https://aclanthology.org/P17-1147>.
- 625
- 626 G Kamradt. Needle in a haystack–pressure testing llms, 2023.
- 627
- 628 Sehoon Kim, Sheng Shen, David Thorsley, Amir Gholami, Woosuk Kwon, Joseph Hassoun, and  
 629 Kurt Keutzer. Learned token pruning for transformers. In *Proceedings of the 28th ACM SIGKDD  
 Conference on Knowledge Discovery and Data Mining*, pp. 784–794, 2022.
- 630
- 631 Tomáš Kočiský, Jonathan Schwarz, Phil Blunsom, Chris Dyer, Karl Moritz Hermann, Gábor Melis,  
 632 and Edward Grefenstette. The NarrativeQA reading comprehension challenge. *Transactions of  
 633 the Association for Computational Linguistics*, 6:317–328, 2018. doi: 10.1162/tacl\_a\_00023.  
 634 URL <https://aclanthology.org/Q18-1023>.
- 635
- 636 Woosuk Kwon, Zhuohan Li, Siyuan Zhuang, Ying Sheng, Lianmin Zheng, Cody Hao Yu, Joseph E.  
 637 Gonzalez, Hao Zhang, and Ion Stoica. Efficient memory management for large language model  
 638 serving with pagedattention. In *Proceedings of the ACM SIGOPS 29th Symposium on Operating  
 Systems Principles*, 2023.
- 639
- 640 Yaniv Leviathan, Matan Kalman, and Y. Matias. Fast inference from transformers via speculative  
 641 decoding. In *International Conference on Machine Learning*, 2022. URL <https://api.semanticscholar.org/CorpusID:254096365>.
- 642
- 643 Yuhong Li, Yingbing Huang, Bowen Yang, Bharat Venkitesh, Acyr Locatelli, Hanchen Ye, Tianle  
 644 Cai, Patrick Lewis, and Deming Chen. Snapkv: Llm knows what you are looking for before  
 645 generation, 2024. URL <https://arxiv.org/abs/2404.14469>.
- 646
- 647 Tianyang Liu, Canwen Xu, and Julian McAuley. Repobench: Benchmarking repository-level code  
 auto-completion systems, 2023.

- 648 Zichang Liu, Aditya Desai, Fangshuo Liao, Weitao Wang, Victor Xie, Zhaozhuo Xu, Anastasios  
 649 Kyriillidis, and Anshumali Shrivastava. Scissorhands: Exploiting the persistence of importance  
 650 hypothesis for llm kv cache compression at test time. *Advances in Neural Information Processing*  
 651 *Systems*, 36, 2024.
- 652 Piotr Nawrot, Adrian Łaniczki, Marcin Chochowski, David Tarjan, and Edoardo M Ponti. Dy-  
 653 namic memory compression: Retrofitting llms for accelerated inference. *arXiv preprint*  
 654 *arXiv:2403.09636*, 2024.
- 655 Zhuoshi Pan, Qianhui Wu, Huiqiang Jiang, Menglin Xia, Xufang Luo, Jue Zhang, Qingwei Lin,  
 656 Victor Ruhle, Yuqing Yang, Chin-Yew Lin, H. Vick Zhao, Lili Qiu, and Dongmei Zhang.  
 657 LLMLingua-2: Data distillation for efficient and faithful task-agnostic prompt compression.  
 658 *ArXiv preprint*, abs/2403.12968, 2024. URL <https://arxiv.org/abs/2403.12968>.
- 659 David Raposo, Sam Ritter, Blake Richards, Timothy Lillicrap, Peter Conway Humphreys, and  
 660 Adam Santoro. Mixture-of-depths: Dynamically allocating compute in transformer-based lan-  
 661 guage models. *arXiv preprint arXiv:2404.02258*, 2024.
- 662 Liliang Ren, Yang Liu, Shuohang Wang, Yichong Xu, Chenguang Zhu, and Cheng Xiang Zhai.  
 663 Sparse modular activation for efficient sequence modeling. *Advances in Neural Information Pro-*  
 664 *cessing Systems*, 36:19799–19822, 2023.
- 665 Ziteng Sun, Ananda Theertha Suresh, Jae Hun Ro, Ahmad Beirami, Himanshu Jain, Felix Yu,  
 666 Michael Riley, and Sanjiv Kumar. Spectr: Fast speculative decoding via optimal transport.  
 667 In *Workshop on Efficient Systems for Foundation Models @ ICML2023*, 2023. URL <https://openreview.net/forum?id=d0mGsaheuT>.
- 668 Romal Thoppilan, Daniel De Freitas, Jamie Hall, Noam Shazeer, Apoorv Kulshreshtha, Heng-Tze  
 669 Cheng, Alicia Jin, Taylor Bos, Leslie Baker, Yu Du, et al. Lamda: Language models for dialog  
 670 applications. *arXiv preprint arXiv:2201.08239*, 2022.
- 671 Hugo Touvron, Louis Martin, Kevin Stone, Peter Albert, Amjad Almahairi, Yasmine Babaei, Niko-  
 672 lay Bashlykov, Soumya Batra, Prajjwal Bhargava, Shruti Bhosale, Dan Bikel, Lukas Blecher,  
 673 Cristian Canton Ferrer, Moya Chen, Guillem Cucurull, David Esiobu, Jude Fernandes, Jeremy  
 674 Fu, Wenyin Fu, Brian Fuller, Cynthia Gao, Vedanuj Goswami, Naman Goyal, Anthony Hartshorn,  
 675 Saghar Hosseini, Rui Hou, Hakan Inan, Marcin Kardas, Viktor Kerkez, Madian Khabsa, Isabel  
 676 Kloumann, Artem Korenev, Punit Singh Koura, Marie-Anne Lachaux, Thibaut Lavril, Jenya Lee,  
 677 Diana Liskovich, Yinghai Lu, Yuning Mao, Xavier Martinet, Todor Mihaylov, Pushkar Mishra,  
 678 Igor Molybog, Yixin Nie, Andrew Poulton, Jeremy Reizenstein, Rashi Rungta, Kalyan Saladi,  
 679 Alan Schelten, Ruan Silva, Eric Michael Smith, Ranjan Subramanian, Xiaoqing Ellen Tan, Binh  
 680 Tang, Ross Taylor, Adina Williams, Jian Xiang Kuan, Puxin Xu, Zheng Yan, Iliyan Zarov, Yuchen  
 681 Zhang, Angela Fan, Melanie Kambadur, Sharan Narang, Aurelien Rodriguez, Robert Stojnic,  
 682 Sergey Edunov, and Thomas Scialom. Llama 2: Open foundation and fine-tuned chat models,  
 683 2023. URL <https://arxiv.org/abs/2307.09288>.
- 684 Harsh Trivedi, Niranjan Balasubramanian, Tushar Khot, and Ashish Sabharwal. MuSiQue: Multi-  
 685 hop questions via single-hop question composition. *Transactions of the Association for Compu-*  
 686 *tational Linguistics*, 2022.
- 687 Georgy Tyukin, Gbetondji J-S Dovonon, Jean Kaddour, and Pasquale Minervini. Attention is all  
 688 you need but you don't need all of it for inference of large language models, 2024. URL <https://arxiv.org/abs/2407.15516>.
- 689 Jason Wei, Yi Tay, Rishi Bommasani, Colin Raffel, Barret Zoph, Sebastian Borgeaud, Dani Yo-  
 690 gatama, Maarten Bosma, Denny Zhou, Donald Metzler, Ed H. Chi, Tatsunori Hashimoto, Oriol  
 691 Vinyals, Percy Liang, Jeff Dean, and William Fedus. Emergent abilities of large language models,  
 692 2022. URL <https://arxiv.org/abs/2206.07682>.
- 693 Thomas Wolf, Lysandre Debut, Victor Sanh, Julien Chaumond, Clement Delangue, Anthony Moi,  
 694 Pierric Cistac, Tim Rault, Rémi Louf, Morgan Funtowicz, Joe Davison, Sam Shleifer, Patrick  
 695 von Platen, Clara Ma, Yacine Jernite, Julien Plu, Canwen Xu, Teven Le Scao, Sylvain Gug-  
 696 ger, Mariama Drame, Quentin Lhoest, and Alexander M. Rush. Transformers: State-of-the-art  
 697 2021.

- 702 natural language processing. In *Proceedings of the 2020 Conference on Empirical Methods in*  
 703 *Natural Language Processing: System Demonstrations*, pp. 38–45, Online, October 2020. As-  
 704 *sociation for Computational Linguistics*. URL <https://www.aclweb.org/anthology/2020.emnlp-demos.6>.
- 705  
 706 Guangxuan Xiao, Yuandong Tian, Beidi Chen, Song Han, and Mike Lewis. Efficient streaming lan-  
 707 guage models with attention sinks, 2024. URL <https://arxiv.org/abs/2309.17453>.
- 708  
 709 An Yang, Baosong Yang, Binyuan Hui, Bo Zheng, Bowen Yu, Chang Zhou, Chengpeng Li,  
 710 Chengyuan Li, Dayiheng Liu, Fei Huang, Guanting Dong, Haoran Wei, Huan Lin, Jialong Tang,  
 711 Jialin Wang, Jian Yang, Jianhong Tu, Jianwei Zhang, Jianxin Ma, Jianxin Yang, Jin Xu, Jin-  
 712 gren Zhou, Jinze Bai, Jinzheng He, Junyang Lin, Kai Dang, Keming Lu, Keqin Chen, Kexin  
 713 Yang, Mei Li, Mingfeng Xue, Na Ni, Pei Zhang, Peng Wang, Ru Peng, Rui Men, Ruize Gao,  
 714 Runji Lin, Shijie Wang, Shuai Bai, Sinan Tan, Tianhang Zhu, Tianhao Li, Tianyu Liu, Wen-  
 715 bin Ge, Xiaodong Deng, Xiaohuan Zhou, Xingzhang Ren, Xinyu Zhang, Xipin Wei, Xuancheng  
 716 Ren, Xuejing Liu, Yang Fan, Yang Yao, Yichang Zhang, Yu Wan, Yunfei Chu, Yuqiong Liu,  
 717 Zeyu Cui, Zhenru Zhang, Zhifang Guo, and Zhihao Fan. Qwen2 technical report, 2024a. URL  
 718 <https://arxiv.org/abs/2407.10671>.
- 719  
 720 Dongjie Yang, XiaoDong Han, Yan Gao, Yao Hu, Shilin Zhang, and Hai Zhao. Pyramidinfer:  
 721 Pyramid kv cache compression for high-throughput llm inference, 2024b.
- 722  
 723 Zhilin Yang, Peng Qi, Saizheng Zhang, Yoshua Bengio, William W. Cohen, Ruslan Salakhutdinov,  
 724 and Christopher D. Manning. HotpotQA: A dataset for diverse, explainable multi-hop question  
 725 answering. In *Conference on Empirical Methods in Natural Language Processing (EMNLP)*,  
 2018.
- 726  
 727 Ann Yuan, Andy Coenen, Emily Reif, and Daphne Ippolito. Wordcraft: story writing with large lan-  
 728 guage models. In *Proceedings of the 27th International Conference on Intelligent User Interfaces*,  
 pp. 841–852, 2022.
- 729  
 730 Amir Zandieh, Insu Han, Vahab Mirrokni, and Amin Karbasi. Subgen: Token generation in sublin-  
 731 ear time and memory, 2024. URL <https://arxiv.org/abs/2402.06082>.
- 732  
 733 Tianyi Zhang, Faisal Ladha, Esin Durmus, Percy Liang, Kathleen McKeown, and Tatsunori B.  
 734 Hashimoto. Benchmarking large language models for news summarization, 2023a. URL <https://arxiv.org/abs/2301.13848>.
- 735  
 736 Zhenyu Zhang, Ying Sheng, Tianyi Zhou, Tianlong Chen, Lianmin Zheng, Ruisi Cai, Zhao Song,  
 737 Yuandong Tian, Christopher Ré, Clark Barrett, Zhangyang Wang, and Beidi Chen. H<sub>2</sub>O: Heavy-  
 738 hitter oracle for efficient generative inference of large language models, 2023b. URL <https://arxiv.org/abs/2306.14048>.

739  
 740 **6 APPENDIX**

741 **6.1 ADDITIONAL ANALYSIS OF FTP**

742 **6.1.1 RESULTS ON L-EVAL**

743 We conduct additional experiments on the L-Eval (An et al., 2023) benchmark for a comprehensive  
 744 evaluation. L-Eval has two groups of tasks: closed-ended tasks and open-ended tasks. The former  
 745 group focus on evaluating an LLM’s ability of reasoning and understanding a long context, while  
 746 the latter one is more about summarization tasks for a long document. We run FTP and Pyramid-  
 747 Infer (Yang et al., 2024b) on the Llama3-8B-Instruct and Qwen2-7B-Instruct models for both tasks,  
 748 and the results are in Table 4 and Table 5 respectively.

749 For closed-ended tasks, FTP with the Llama3 model sustains considerable performance across half  
 750 of the datasets, and achieves a TTFT speedup comparable to PyramidInfer. When applied on Qwen2-  
 751 7B-Instruct model, FTP not only enhances the performance on the GSM (Cobbe et al., 2021) and  
 752 CodeU datasets, but also surpasses the baseline scores. Furthermore, the longer context length for  
 753 Qwen2 illustrates the acceleration of FTP during the prefilling stage, showcasing its efficiency.

For open-ended tasks, we employ GPT4 as a judge to compare the outputs from the model with those from GPT-3.5-turbo-16k-0613. Each pair of predictions is evaluated by GPT4 twice, with their positions swapped after the first judgement. The number of wins and ties for the model are recorded in Table 5. As illustrated in the results, FTP achieves higher TTFT speedup for both models, and notably, the performance on Qwen2-7B-Instruct even surpasses that of the baseline.

Model	Coursera	GSM	QuALITY	CodeU	SFiction	TRL	TPO	Avg.	SpeedUp
Llama3 Baseline	52.76	<b>66.00</b>	<b>60.40</b>	<b>4.44</b>	<b>71.09</b>	<b>62.00</b>	75.46	<b>56.02</b>	1.00
Llama3 + FTP	<b>53.20</b>	38.00	55.45	4.44	69.53	52.00	74.35	49.57	1.21
Llama3 + PyramidInfer	52.18	68.00	60.40	4.44	71.09	49.33	<b>75.84</b>	54.47	<b>1.24</b>
Qwen2 Baseline	68.60	24.00	<b>65.35</b>	7.78	<b>73.44</b>	<b>47.33</b>	<b>81.04</b>	52.51	1.00
Qwen2 + FTP	68.60	<b>30.00</b>	65.35	<b>10.00</b>	72.66	43.33	80.30	<b>52.89</b>	<b>2.50</b>
Qwen2 + PyramidInfer	<b>69.77</b>	30.00	65.35	6.67	71.88	42.67	81.04	52.48	2.01

Table 4: L-Eval results on closed-ended tasks. “TRL” stands for the “topic retrieval longchat” dataset, and “SpeedUp” represents the TTFT speedup w.r.t. the baseline.

Model	Wins	Ties	Win-rate (%)	TTFT SpeedUp
Llama3 Baseline	50	62	<b>42.19</b>	1.00
Llama3 + FTP	44	67	40.36	<b>1.19</b>
Llama3 + PyramidInfer	49	51	38.80	1.08
Qwen2 Baseline	42	75	42.97	1.00
Qwen2 + FTP	47	69	<b>43.58</b>	<b>1.21</b>
Qwen2 + PyramidInfer	35	69	37.37	1.09

Table 5: L-Eval results on open-ended tasks. The output of models are compared with that of GPT-3.5-turbo-16k-0613 by the judge model (*i.e.*, GPT4).

### 6.1.2 NEEDLE-IN-A-HAYSTACK EVALUATION

In this section, we evaluate whether FTP results in the loss of intermediate information by conducting the Needle-in-a-Haystack (Kamradt, 2023) experiment. The Needle-in-a-Haystack test inserts a specific statement (referred to as the “needle”) in the middle of a long-context document (the “haystack”), and requires the LLM to retrieve this statement. For evaluation, a GPT4 (Achiam et al., 2023) model is utilized to score the relevance between the LLM’s output and the “needle”.

We iterate the context length from 1000 to the max context length of the model, and position the “needle” from the beginning (0.0%) to the end (100%) in steps of 10% for each context length. The result for the Llama3-8B-Instruct and Qwen2-7B-Instruct models are presented in Figure 8. As demonstrated in the results, the Qwen2 baseline model exhibits substantial retrieval capabilities. Our method appears to have minimal impact on this feature, successfully retrieve the “needle” across nearly all context lengths and depths of the “needle”. For the Llama3 model, FTP even enhances performance as the context length approaches its limit. The results in Figure 8 suggest that FTP does not lead to a loss, and may even reduce the loss of intermediate information.

### 6.1.3 THE IMPACT OF INITIAL AND THE LAST TOKENS

In this section, we tune the hyper-parameters  $P$  and  $N$  mentioned in Section 3.2.1 to analyse their impact on model accuracy. The experiments are conducted on the Qasper (Dasigi et al., 2021) HotpotQA (Yang et al., 2018) dataset, with a Llama3-8B-Instruct model,  $\mathcal{F} = 10$  and  $\eta = 0.95$ , and the results are in Table 6. The results demonstrates that choosing an excessively small  $P$  or  $N$  yields significant decrease in accuracy, although they reduce the computational overhead of FTP. Nonetheless, an increase in  $P$  or  $N$  does not necessarily translate to improved accuracy. Moreover, a larger  $N$  typically incurs additional computational cost and results in a reduced number of pruned tokens given the same  $\eta$ .

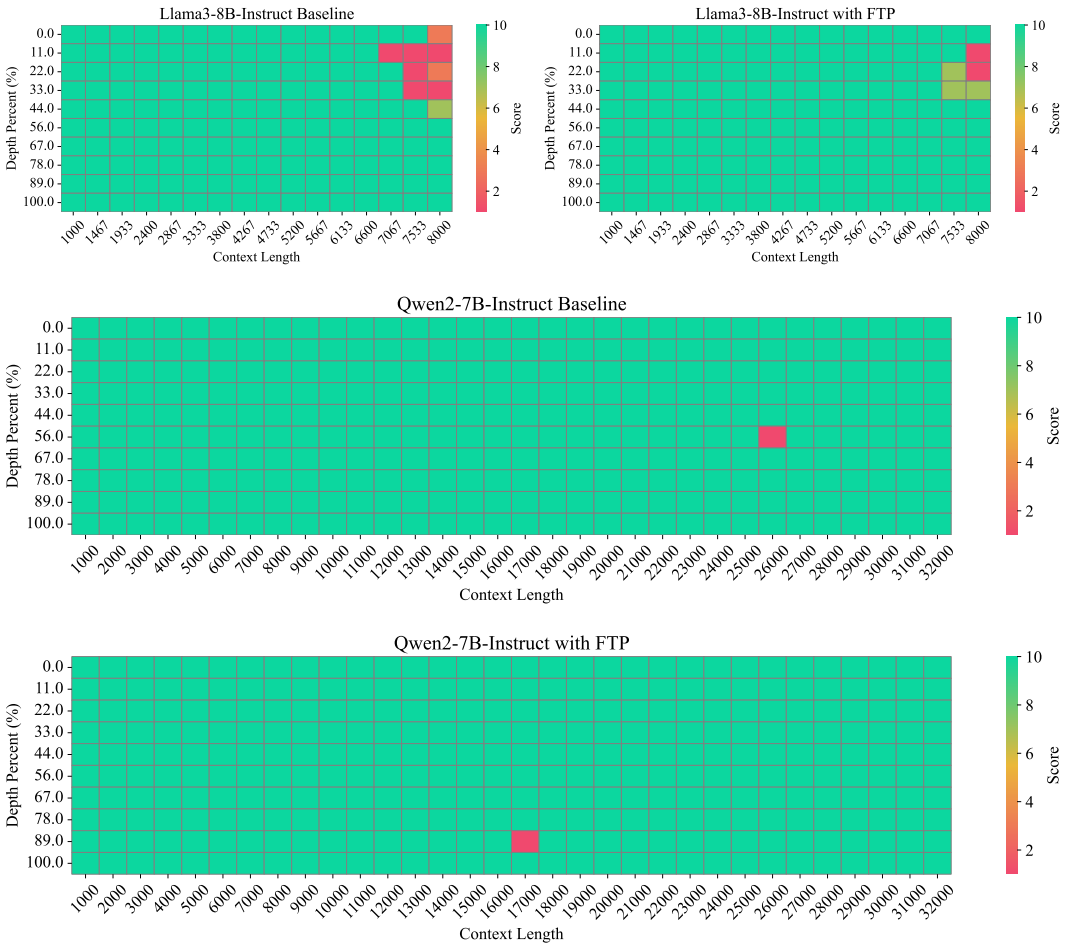


Figure 8: Visualization of the result of the Needle-in-a-Haystack test for Llama3-8B-Instruct and Qwen2-7B-Instruct with and without FTP. The x-axis represents the length of the documents and the y-axis denotes the position of the statement “needle”. The scores are given by GPT4 (Achiam et al., 2023) by evaluating the relevance of the model output and the “needle”.

P \ N	1	10	20	50	80	100	150	200
1	34.99	43.16	43.80	42.74	41.74	42.44	43.49	42.99
10	37.25	42.44	45.34	45.11	45.14	44.90	44.89	45.40
20	37.38	42.44	45.50	45.06	44.93	45.19	44.36	44.41
50	36.77	42.67	45.40	44.75	44.61	44.95	43.73	45.03
80	37.26	43.05	44.95	45.27	45.11	44.73	45.24	43.85
100	38.13	43.44	44.81	45.75	44.92	45.46	44.94	44.39
150	37.27	43.05	44.51	44.57	45.08	45.67	45.25	45.61
200	38.46	42.87	44.78	45.00	45.38	45.43	44.88	45.01

Table 6: Accuracy score under different settings of the initial and the last reserved tokens. The scores are averaged over Qasper and HotpotQA datasets.

#### 6.1.4 RESERVED RATIOS

We also conduct experiments to analyse the impact of the reserved ratio  $\eta$  for FTP as mentioned in Section 3.2.1. We statically reserve the first  $F = 10$  layers and set different reserved ratios  $\eta$  for the subsequent layers of the Qwen2-7B-Instruct model. The experiments are conducted on LongBench

Tasks	$\eta = 0.65$	$\eta = 0.70$	$\eta = 0.75$	$\eta = 0.80$	$\eta = 0.85$	$\eta = 0.90$	$\eta = 0.95$
Single-Document QA	33.20	34.13	34.96	36.46	36.79	37.23	38.75
Multi-Document QA	29.69	30.28	30.53	32.24	34.23	34.60	35.21
Summarization	21.22	21.43	21.90	22.63	23.34	24.25	25.01
Few-shot Learning	64.13	64.29	65.17	66.08	68.20	67.34	69.11
Synthetic	25.00	29.00	31.75	33.25	35.75	34.50	36.75
Code Completion	50.22	50.92	52.35	54.14	53.97	56.08	56.74

Table 7: The accuracy score for each task in LongBench when applying different reserved ratios  $\eta$  for FTP on the Qwen2-7B-Instruct model.

and the results of accuracy score and TTFT speedup are shown in Table 7 and Table 8 respectively. As shown in the results, FTP has a considerable TTFT speedup even when  $\eta$  is set to 0.95, suggesting a substantial number of tokens are pruned. More importantly, as  $\eta$  is progressively reduced from 0.95 to 0.65, the speedup continues to increase, but the rate of increment in speedup gradually becomes smaller. This observation is consistent with our analysis in Section 3.2.2 and Figure 6. However, the decrease in accuracy does not follow this pattern. Therefore, FTP can achieve an optimal balance between accuracy and TTFT speedup when  $\eta$  is approximately 0.80.

Tasks	$\eta = 0.65$	$\eta = 0.70$	$\eta = 0.75$	$\eta = 0.80$	$\eta = 0.85$	$\eta = 0.90$	$\eta = 0.95$
Single-Document QA	1.49	1.47	1.45	1.41	1.37	1.32	1.22
Multi-Document QA	1.54	1.52	1.49	1.46	1.42	1.36	1.26
Summarization	1.48	1.46	1.44	1.41	1.37	1.31	1.23
Few-shot Learning	1.50	1.48	1.46	1.43	1.40	1.35	1.25
Synthetic	1.55	1.54	1.52	1.50	1.46	1.40	1.30
Code Completion	1.48	1.45	1.44	1.41	1.37	1.32	1.22

Table 8: The TTFT speedup ( $\times$ ) for each task in LongBench when applying different reserved ratio  $\eta$  for FTP on the Qwen2-7B-Instruct model.

### 6.1.5 RESERVED LAYERS

In this section, we explore the impact of reserving shallow layers as mentioned in Section 3.2.2. We set different  $\mathcal{F}$  to reserve different numbers of shallow layers and fix  $\eta$  to 0.90 for the following layers of Qwen2-7B-Instruct when applying FTP. The experiments are conducted on LongBench and the results of accuracy score and TTFT speedup are presented in Table 9 and Table 10 respectively. As shown in the results, the accuracy score increases as more shallow layers of the model are fully reserved. However, some certain tasks (*e.g.*, Few-Shot Learning and Synthetic) exhibit little changes in accuracy score or even demonstrate an increase in accuracy when  $\mathcal{F}$  is incremented from 5 to 10. In general, the TTFT speedup increases as we decrease  $\mathcal{F}$ . However, there is an anomalous decline in speedup when  $\mathcal{F}$  is reduced from 10 to 9. This anomaly could be explained by a change to the distribution of attention weights to a more uniform pattern at  $\mathcal{F} = 9$  compared to  $\mathcal{F} = 10$ , resulting in a decrease in the number of pruned tokens.

Tasks	$\mathcal{F} = 4$	$\mathcal{F} = 5$	$\mathcal{F} = 6$	$\mathcal{F} = 7$	$\mathcal{F} = 8$	$\mathcal{F} = 9$	$\mathcal{F} = 10$
Single-Document QA	33.70	33.99	36.00	35.73	36.56	36.81	37.23
Multi-Document QA	31.68	31.72	32.44	32.65	32.23	33.30	34.60
Summarization	22.24	22.61	22.69	22.95	23.38	23.78	24.25
Few-shot Learning	65.67	67.38	67.74	67.82	67.32	67.38	67.34
Synthetic	32.25	35.75	34.50	33.25	38.00	36.25	34.50
Code Completion	52.98	53.20	53.93	54.70	54.79	55.82	56.08

Table 9: The accuracy score for each task in LongBench when reserving different numbers of shallow layers for FTP on the Qwen2-7B-Instruct model.

Tasks	$\mathcal{F} = 4$	$\mathcal{F} = 5$	$\mathcal{F} = 6$	$\mathcal{F} = 7$	$\mathcal{F} = 8$	$\mathcal{F} = 9$	$\mathcal{F} = 10$
Single-Document QA	1.42	1.40	1.39	1.37	1.35	1.30	1.32
Multi-Document QA	1.47	1.45	1.43	1.42	1.40	1.35	1.36
Summarization	1.42	1.41	1.39	1.37	1.36	1.30	1.31
Few-shot Learning	1.47	1.44	1.42	1.41	1.39	1.34	1.35
Synthetic	1.51	1.50	1.48	1.47	1.45	1.40	1.40
Code Completion	1.42	1.41	1.39	1.37	1.36	1.30	1.32

Table 10: The TTFT speedup ( $\times$ ) for each task in LongBench when reserving different numbers of shallow layers for FTP on the Qwen2-7B-Instruct model.

## 6.2 ADDITIONAL VISUALIZATION OF ATTENTION WEIGHTS

To illustrate the generalizability of our findings discussed in Section 3.2.1, we visualize the attention weights of more samples from the Qasper (Dasigi et al., 2021) dataset, as presented in Figure 9.

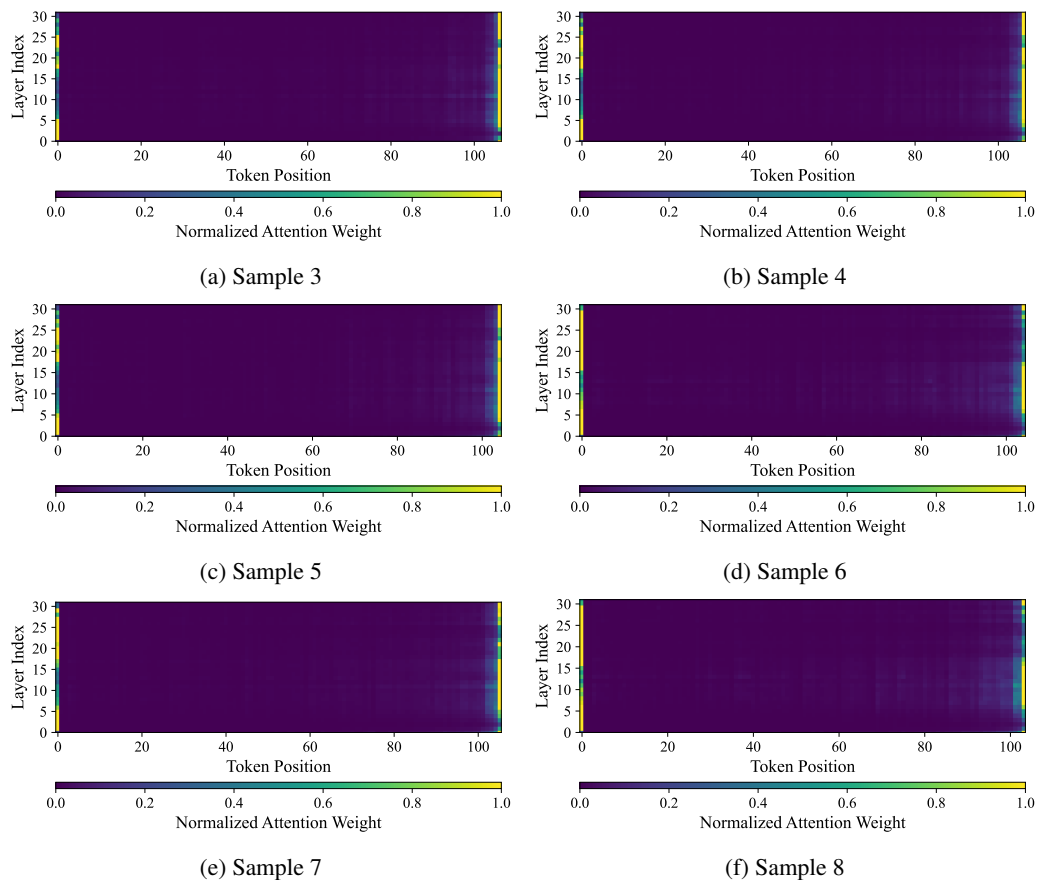


Figure 9: Additional visualization of the normalized attention weight for each layer. The experiment is conducted on a Llama3-8B-Instruct model on the Qasper dataset. Since the input length is too long to visualize, we divide the tokens into several groups with a group size of 32. Each column in the graph represents the average attention weight of a group of tokens across all layers.